Innovative insights in a plug flow microreactor for operando X-ray studies

Santiago Figueroa, Dean Gibson, Trevor Mairs, Sébastien Pasternak, Mark Newton, Marco Di Michiel, Jérome Andrieux, Konstantinos Christoforidis, Ana Iglesias-Juez, Marcos Fernández-García, et al.

Contact person for this submission: Santiago J. A. Figueroa
(santiago.figueroa@lnls.br; phone: 00551935175063; fax: 00551935121004)

Innovative insights in plug flow microreactor for *operando* X-ray studies

Santiago J. A. Figueroa[a1]*, Dean Gibson[a], Trevor Mairs[a], Sebastien Pasternak[a], Mark A. Newton[a], Marco Di Michiel[a], Jerome Andrieux[a2], Konstantinos C. Christoforidis[b], Ana Iglesias-Juez[b], Marcos Fernández-García[b] and Carmelo Prestipino[c]

[a]European Synchrotron Radiation Facility, Jules Horowitz 6/BP220, Grenoble, 38043, France, [b]Instituto de Catálisis y Petroleoquímica, CSCI, Marie Curie 2, Cantoblanco, Madrid, 28049, Spain, and [c]Institute Sciences Chimiques de Rennes UMR 6226, CNRS, Campus de Beaulieu, Rennes, 35042, France

Correspondence email: santiago.figueroa@lnls.br

[1] Current Address: Centro Nacional de Pesquisa em Energia e Materiais (CNPEM), Laboratório Nacional de Luz Síncrotron (LNLS), Rua Giuseppe Maximo Scolfaro, 10.000, Polo II de Alta Tecnologia, Caixa Postal 6192, 13083-970 Campinas, SP (Brazil)

[2] Current Address: Universite Claude Bernard Lyon 1, 43 Boulevard du 11 novembre 1918, 69622 Villeurbanne-Cedex, Lyon (France).

Keywords: operando X-ray studies; plug flow microreactors; in situ; catalysis.

Synopsis

We minimized temperature gradients in a plug flow microreactor by means of an aluminum shield. The goal was reached by focusing the infrared radiation on the catalyst bed. The overall efficiency of the reactor was improved at high temperatures.

Abstract

Different solutions have been proposed over the years to optimize the temperature and atmosphere control over a catalyst in order to reach an ideal reactor behavior. Here**,** a new, innovative solution aiming to minimize temperature gradients along the catalyst bed is shown. This goal was reached by focusing the infrared radiation generated from the heating elements onto the catalyst bed with the aid of an aluminum shield. This solution yields ~0.13 K/mm axial temperature gradients ranging from 960 up to 1173 K and with adequate capillaries, pressure could reach at least 20 bar.

1. Introduction

There is an increasing importance attached to the application of *operando* techniques to study heterogeneous catalysis in order to explore the often complex structure-property relationships. It should be understood that only by measuring the reactant conversion or the product formation rate you can be sure that the catalysts behave and perform as expected. Moreover**,** as the surface and sometimes the bulk structure of catalysts can be modified under reaction conditions, the use of techniques such as spectroscopies or diffraction are required, enabling us to investigate catalysts under the actual conditions of operation. This kind of characterization enhances our overall understanding of the catalytic process, allows a direct correlation between the catalyst properties and the activity and/or selectivity, and provides clues to determine the active reaction sites/phases.

The core of an X-ray *operando* study is the reaction cell holding the catalyst in the X-ray beam**,** which makes it possible to specify and control the reactant flow to the catalyst. Since Clausen *et al.* (1991) introduced the first XRD adapted plug flow reactor, many variants on this overall theme have occurred (Li *et al.*, 2001; Grunwaldt *et al.*, 2004; Bare *et al.*, 2007; Chupas *et al.*, 2008; van Beek *et al.*, 2011). However, as Meunier and others have already realized, spectroscopic cells are not usually ideal catalytic reactors (Meunier, 2010) for several reasons, such as the temperature gradients (axial and radial) along the catalyst bed, and components that may by themselves be unstable or reactive under reaction conditions. To avoid the latter, the reactor itself must not contain any element that can be catalytically active. To address the issue of isothermality and temperature gradients we propose an innovative idea that has come out by working in the plug flow microreactor model proposed by Chupas *et al*. (2008). This initial design was rebuilt, primarily to make dispersive EXAFS studies more tenable but also to improve overall usability aspects.

To diminish the presence of any thermal gradients a circular aluminum shield has been implemented within the heating system and around the capillary itself. Aluminum reflects infrared (IR) light extremely well. By combining this property with an appropriate geometry that focuses the radiation onto the catalyst bed this configuration is able to minimize axial temperature gradients along the bed at high temperatures, reaching values of ~0.13 K/mm under working conditions. The aluminum shield has appropriate cut-outs for the incoming and transmitted X-rays that are optimized for performing experiments in transmission and fluorescence geometries, while the incorporation of the shield does not compromise the performance of the reactor for total scattering studies which was the original purpose of this design. The background scattering contribution derived from the shield is negligible and easily discardable, and therefore this design may be used for experiments that are sensitive to parasitic X-ray scattering.

The addition of a second capillary in this cell was originally a result of considering applications involving dispersive EXAFS wherein a suitable reference is required to obtain EXAFS from certain

types of material (Newton, 2007). However, the addition of this second tube has been also useful for other reasons: for instance, this can be used to allow the measurement of references or two simultaneous thermal treatments during variable temperature measurements increasing the overall efficiency of experimentation time. The catalytic properties, together with activity, selectivity and stability, can be evaluated during the structural and electronic characterization by using a mass spectrometer or a micro gas chromatograph installed in the microreactor outlet. According to our lab tests we are able to perform flow pressure measures of up to 20 bars. Consequently, this cell allows us to conduct *operando* experiments on working powder catalysts under industrially relevant conditions (Bare *et al.*, 2011).

2. Cell Description and performance

As illustrated in Fig. 1 the reactor is built using modular components that are sufficiently robust so as to give the necessary assembly flexibility. The oven itself is mounted in a 50 mm square aluminum profile which also contains two support welded Swagelok fittings (1/8´´ Swagelok). One of these supports is permanently fixed, corresponding to the exhaust part of the reactor. It consists of a T-piece holding a thermocouple that can be placed inside the capillary close to the sample as shown in Fig. 1. In order to optimize flow, decrease dead volumes, and make the radial gradients along the bed negligible, we have attempted to minimize all the possible flow dimensions (Meunier, 2010). For this reason, we use up to 1.6 mm external diameter quartz capillaries. The wall thickness is selected depending on the X-ray energy used and the pressure range required for the measurement. The usual thickness ranges from 0.01 up to 0.2 mm; the combination of thin capillary walls and small sample volumes is crucial to achieve a good heat transmission and allow a finely controllable heating environment (Jacques *et al.*, 2009).

For low temperature operation (max 673 K) the use of kapton capillaries is viable. The catalyst powder is adequately sieved (Jacques *et al.*, 2009) and placed in between two quartz wool plugs to prevent blow out during operation. At this stage we slide the capillary into the thermocouple as close to the bed as possible (1 mm or less) and glue the capillary into the stainless steel tubes with a high temperature epoxy glue (van Beek *et al.*, 2011). This solution prevents air leaks and avoids any unnecessary mechanical tension on the capillaries derived from the use of ferrules, which is the main source of capillary failure in such arrangements. The movable support separation is easily displaced to accommodate capillaries of different length. Now the aluminum shield may be shifted in the profile, thus enabling it to be placed over the sample and aligned by a simple movement. Heating is supplied by Kanthal A-1 resistive heaters (as described in Chupas *et al.*, 2008) mounted inside the aluminum shield, coiled around a ceramic tube and connected in parallel to the power supply via porcelain insulators. Power is provided by a DC power supply (Delta Elektronika SM70-AR-24), regulated by an Eurotherm 2400 temperature controller based on the sample temperature measured by the K type

thermocouple (0.25mm or 0.5mm). The thermocouple size has been chosen in order to minimize the heat transfer that can be provided to the catalyst but at the same time assures enough temperature stable gauge for the exothermic or endothermic reaction. For the cases studied here, capillaries from 0.5mm up to 1mm were paired with 0.25mm size thermocouples (Omega Engineering Inc., Model KMTIN-010U-6, 0.25mm), and for capillaries from 1.1mm up to 1.6mm, a 0.5mm size thermocouple (Omega Engineering Inc., Model KMTIN-020U-6, 0.5mm) was used.

As previously noted, aluminum has one of the best reflectivity coefficients for medium and far infrared radiation (as much as 98%) (Wolfe & Zissis, 1993) and the capillaries are held at the center of the cylindrical hole cut into the aluminum piece. This allows focusing the infrared directly onto the capillary. The maximum working temperature reached exceeds the melting point of Aluminum (933 K) but, as experimentally verified, the temperature on the shield does not exceed 500 K at the maximum working temperature; this being an effect of the shield´s reflective properties. The shield is further covered with a kapton window to minimize convection cooling. As additional benefits, the Electrical Power and the time response required to achieve a given target temperature is significantly reduced compared with the case where no aluminum shield is found.

As illustrated in Fig. 2, the thermal gradient along 8 mm bed decreases when the temperature increases. This effect can be understood by keeping in mind that heat transfer is dominated at low temperatures by natural convection, from higher (heaters) to lower temperatures regions (kapton window) and at high temperatures the heat transfer is dominated by radiant heat transfer. So, the current use effectiveness of an IR reflective element increases with temperature and therefore the temperature becomes more stable at higher temperatures when the heat transfer regime is close enough to be fully radiant (Rohsenow & Choi, 1961). With this design the axial thermal gradient along the bed was measured to ~0.13 K/mm at high temperatures under working conditions (space velocity of 15000h^{-1} in a 1mm-diameter capillary with 0.025mm wall thickness at temperatures ranging from 960 K up to 1173 K). This value is a bit lower than the one claimed by Clausen *et al.* (1991) of ~0.15 K/mm (3K in 20mm, using a gas blower as heating system) but unfortunately in their estimation is not clear: the wall thickness of the capillary used, if is measured in flow and up to which temperature this claimed gradient is valid, thus turning difficult to perform an accurate comparative analysis between these two different heating systems.

In order to compare the catalytic performance of the X-ray microreactor with a conventional laboratory reactor, the CO conversion in the water gas shift reaction obtained by a 12 wt.% CeO_2 in 10 wt.% Cu/Al_2O_3 reforming catalyst was measured four times at four different temperatures (see supplementary information for more experimental details) and it can be shown in Fig. 3. As quoted above, the differences in the conversion profile are less than 4% for both the X-ray microreactor and the laboratory reactor. Taking into account the associate error of the value estimation, the measures

are comparable. Differences can be ascribed not to temperature, but due to gas diffusion differences through the bed. Thus, the goal of achieving an in situ X-ray reactor design exhibiting close the same conversion and behavior at equivalent residence times to a laboratory reactor has been met with this design for the typical catalytic reaction tested here.

As in their early work Clausen *et al.* (1991) did not expect to be able to estimate the maximum pressure a capillary could support, and based on the work of Tekmen & Müller (2004), a theoretical estimation of the maximum pressure supported by the capillaries was calculated. The quartz capillaries used have a 1mm diameter with a 0.025mm wall thickness. The capillaries are calculated so as to resist 177 bar maximum internal pressures (this including a factor 3 as a safety factor). Consequently, the maximum (theoretical) working pressure, after the safety coefficient application, was ~60 bars. It should be noted that in order to validate the microreactor the experimental test was however restricted to 20 bar.

As comment on the introduction a second capillary tube was incorporated as can be shown in Fig.1 and in more detailed picture at Supplementary Information. This second tube have a independent entrance of gases, power supply and thermocouple, then is able in principle to conduct other reaction simultaneously to the first tube, but this application is actually under development. The commissioned uses of this second capillary are as reference for dispersive EXAFS under supported catalyst or diffraction reference, non simultaneous thermal treatments and eventually can act as substitute oven if there are problems with the first one, as for design the aluminum piece which contain both ovens has inversion symmetry, and then there are completely exchangeable.

3. Applications

Next, we show some brief examples of results obtained by using the microreactor on XANES and XRD in situ experiments under *operando* conditions. Details of sample preparation and of absorption and diffraction setup can be found in Christoforidis *et al.*, 2012*a*,*b*. The studies were carried out on beamlines BM23 (Fe-K edge, Si 111, $\Delta E/E = 2.0 \times 10^{-4}$) and ID15B (86.8 keV, $\lambda = 0.143$ Å, $\Delta E/E = 1{,}4 \times 10^{-3}$) of the ESRF. In this example the catalyst contains a few percentage of iron (1.5% Fe-doped TiO_2). Thus, as we are interested in XAFS in situ experiments using the microreactor, the limitation on maximum capillary size (up to 1.6mm) give us a edge step lower than 0.1 then the experiment must be carried out in fluorescence mode. In this particular case, the choice of an aluminum shield has practical advantages compared to stainless steel or other shields that may have their own intrinsic iron content, and completely avoid any potential interference from any background fluorescence coming from the shield or heaters as experimentally proved. Another advantage of the chosen design is that we can make the X-rays enter at 45 degrees from the front side (Fig.1 Front Picture) collecting simultaneously a transmission and fluorescence spectra. Using the two X-ray

techniques, we have investigated the effect of dopants (sulfur and iron) on local structure modifications and on the process of nucleation and growth of anatase polymorph from amorphous powders. XAFS spectroscopy was applied to study the effect of sulfur on the coordination environment and iron oxidation state in Fe-doped TiO_2 nanomaterials. As a natural result of *operando* experiments we obtain a huge amount of spectra, for this reason XAFS data reduction was performed using *PrestoPronto* (Prestipino & Figueroa, 2010 and Bordiga *et al.* 2013) a special developed code for handling large datasets as the ones that can sort out in time or space resolved experiments coming from Q-EXAFS and dispersive EXAFS beamlines. Figure 4 presents representative Fe K-edge spectra in the XANES region under thermal treatment starting from room temperature up to 973K with 5 $K.min^{-1}$ under dry synthetic air (20% O_2 in He, $10ml.min^{-1}$). As explained in Christoforidis *et al.*, 2012*a* this experimental results show that sulfur does not modify the local geometry and iron oxidation state either in amorphous or crystallized materials. Figure 5 shows in-situ diffraction data of a representative TiO_2 sample under thermal treatment ramp. A mass spectrometer was fitted to the outlet of the flow-microreactor allowing the observation of the gaseous products evolution during the thermal treatment and offering advantages in ascribing the released gaseous products (H_2O, C-, N- and S-based) to specific crystallization steps and/or the burning of organic moieties coming from the aqueous synthesis, these results are in close agreement to those obtained in the laboratory with a conventional reactor given an additional support to the *operando* reactor behavior. The transition from amorphous to well crystalline anatase structure can be observed. The broad diffuse-like features in the XRD pattern, characteristic of the amorphous structure, develop gradually into a well crystallized anatase structure (JCPDS 21-1272). Besides, these in-situ experiments furtherly show that sulfur does not rather affect the nucleation onset but the activation energy of the growth process of anatase polymorphs, influencing the primary particle size and shape of the nanomaterials (Christoforidis *et al.*, 2012*b*). In addition, the microreactor was also used to obtain in-situ time-resolved X-ray total scattering data, as with the original design due to Chupas *et al.* 2008, and by applying pair distribution function (PDF) analysis to obtain local structure information in the amorphous, intermediate and well crystallized states of TiO_2 based materials (Christoforidis *et al.*, 2013).

In summary, the use of a single set-up for obtaining precise short (XAS; PDF-XRD) and long range (PDF-XRD, XRD) information from the solid helps to obtain an unified view of the structural parameters affecting nucleation and growth of a nanomaterial, thus providing key information to allow morphological control. The presence of anion and cation moieties was shown to alter a number of such morphological properties which are considered as key to understand the chemical (e.g. catalytic) properties of the systems (Christoforidis *et al.*, 2012*a,b* and 2013).

4. Conclusions

The design and improvement of versatile plug flow microreactors aiming to achieve, at a laboratory scale, the relevant industrial conditions of chemical processes, are of ongoing development and significance. The development of the microreactor described here opens the possibility for new types of studies combining XAFS/XRD to probe the structural order of short/long range and the kinetics of reaction at temperatures up to 1173K. The correlation in between both experimental techniques is straightforwardly done by using the same reactor. The innovative shield introduced in this new microreactor design effectively ameliorates the thermal gradients along a catalyst bed, yielding increased accuracy/certainty in any given experimental situation. The overall efficiency of the reactor operation is also proportionally improved to high temperatures due to the effect of the shield to focus the radiation to the capillary.

Acknowledgements The authors acknowledge the European Synchrotron Radiation Facility for the provision of beamtime on beamlines ID24, BM23 and ID15. SJAF thanks to Innokenty Kantor for some useful discussions on the model and Hugo Vitoux and Florian Perrin for their contributions on the experiments. The authors gratefully acknowledge the help of Peter J Chupas for providing the technical schematics of their original reactor system developed at Argonne National Laboratory, also Paula Caldas and José Maria Corrêa Bueno (UFSCar-Brazil) for the standard laboratory measures included in Fig.3. The research leading to these results has been funded by the Spanish CICYT (CTQ2010-14872/BQU) and the European Union's Seventh Framework Programme (FP7/2007-2013) under grant agreement n° 253445. Dr. K.C. Christoforidis acknowledges Marie Curie Action – Intra-European Fellowship (FP7-PEOPLE-2009-IEF-253445) for a Post-doctoral Fellowship.

References

Bare, S.R., Yang, N., Kelly, S.D., Mickelson, G.E. & Modica, F.S. (2007). *Cat. Tod.* **126**, 1-2, 18-26.

Bare, S.R., Kelly, S.D. & Mickelson, G.E. (2011) *Synch. Rad. News*, **24**, 6, 12-17.

Bordiga, S., Groppo, E., Agostini G., Van Bokhoven, J. A. & Lamberti, C. (2013). *Chem. Rev.* 113, 1736-1850.

Christoforidis, K.C., Figueroa, S.J.A. & Fernández-García, M. (2012*a*). *Appl. Cat. B*, **117-118**, 310-316.

Christoforidis, K.C., Iglesias-Juez, A., Figueroa, S.J.A., Newton, M.A., Di Michiel, M. & Fernández-García, M. (2012*b*). *Phys . Chem. Chem. Phys.*, **14**, 5628-5634.

Christoforidis, K.C., Iglesias-Juez, A., Figueroa, S.J.A., Di Michiel, M., Newton, M.A. & Fernández-García, M. (2013). *Catal. Sci Technol.*, **3**, 626-634.

Chupas, P. J., Chapman, K.W., Kurtz, C., Hanson, J. C., Lee, P.L. & Grey, C.P. (2008). *J. Appl. Cryst.* **41**, 822-824.

Clausen, B.S., Steffensen, G., Fabius, B., Villadsen, J., Feidenhans, R. & Topsøe, H. (1991). *J. Catal.*, **132**, 524-535.

Grunwaldt, J.-D., Caravati, M., Hannemann, S. & Baiker, A. (2004). *Phys. Chem. Chem. Phys.*, **6**, 3037-3047.

Jacques, S.D.M., Leynaud, O., Strusevich, D., Stukas, P., Barnes, P., Sankar, G., Sheehy, M., O´Brien, M.G., Iglesias-Juez, A. & Beale, A.M. (2009). *Cat. Tod.* **145**, 3-4, 204-212.

Li, S., Meitzner, G.D. & Iglesia, E. (2001) *J. Phys. Chem. B*, **105**, 24, 5743-5750.

Meunier, F.C. (2010). *Chem. Soc. Rev.* **39**, 12, 4602-4614.

Newton, M.A. (2007). *J. Synchrotron Rad.* **14**, 4, 372-381.

Prestipino, C. & Figueroa, S. J. A. (2010) *PrestoPronto*, Available at http://code.google.com/p/prestopronto/

Rohsenow, W.M. & Choi, H. (1961). *Heat Mass and Momentum Transfer*, New York: Prentice Hall.

Tekmen, M. & Müller, J. D. (2004). *Rev. Sci. Instrum.*, **75**, 12, 5143-5148.

van Beek, W., Safonova, O.V., Wiker, G. & Emerich, H. (2011). *Phase Transitions*, **84**, 8, 726-732.

Wolfe, W.L. & Zissis, G.J. Eds., (1993). *The Infrared Handbook*, Environmental Research Institute of Michigan, Ann Arbor, MI.

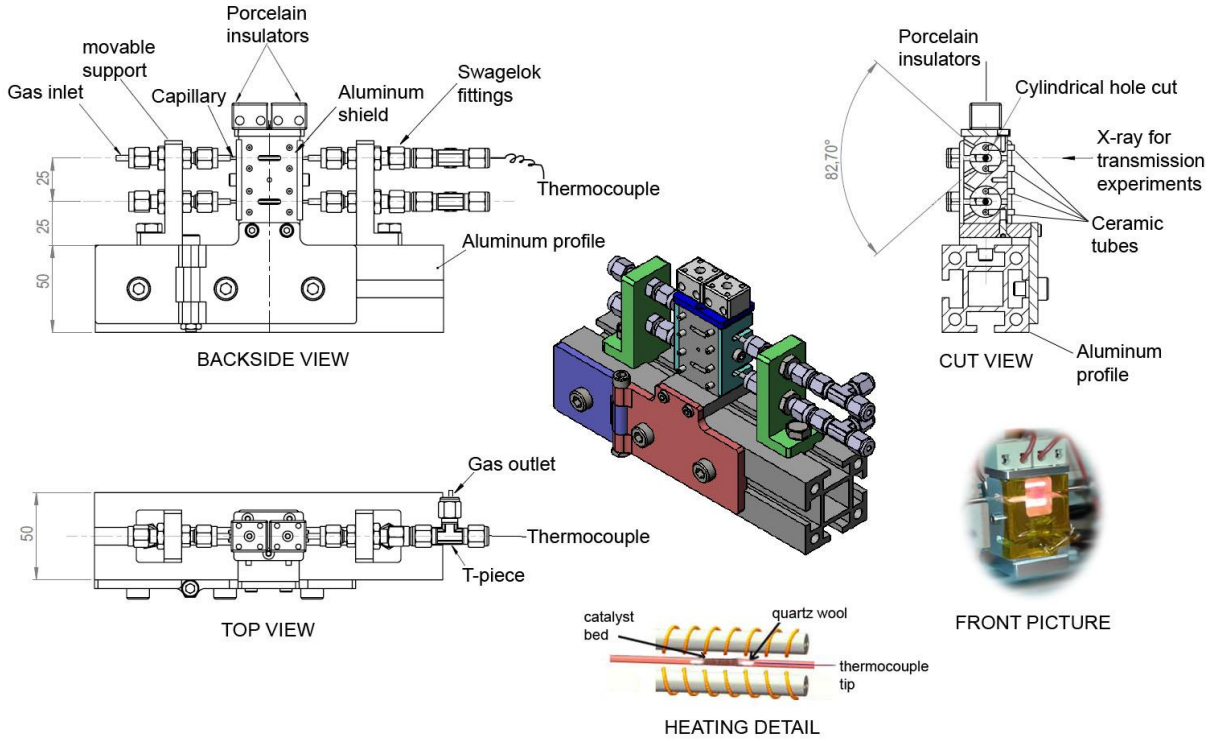

Figure 1 Microreactor technical design and components. At center, in full color, the fully assembled flow-cell/furnace is shown; several different views are sketched (top, backside and a cut view), to facilitate following the text. The heating detail illustrated shows the relative position of the catalyst bed and thermocouple tip in between the quartz wool. The front picture is a photograph of the flow-cell/furnace under working conditions at 1073K, the Kapton tape avoiding air currents that might suddenly change the temperature.

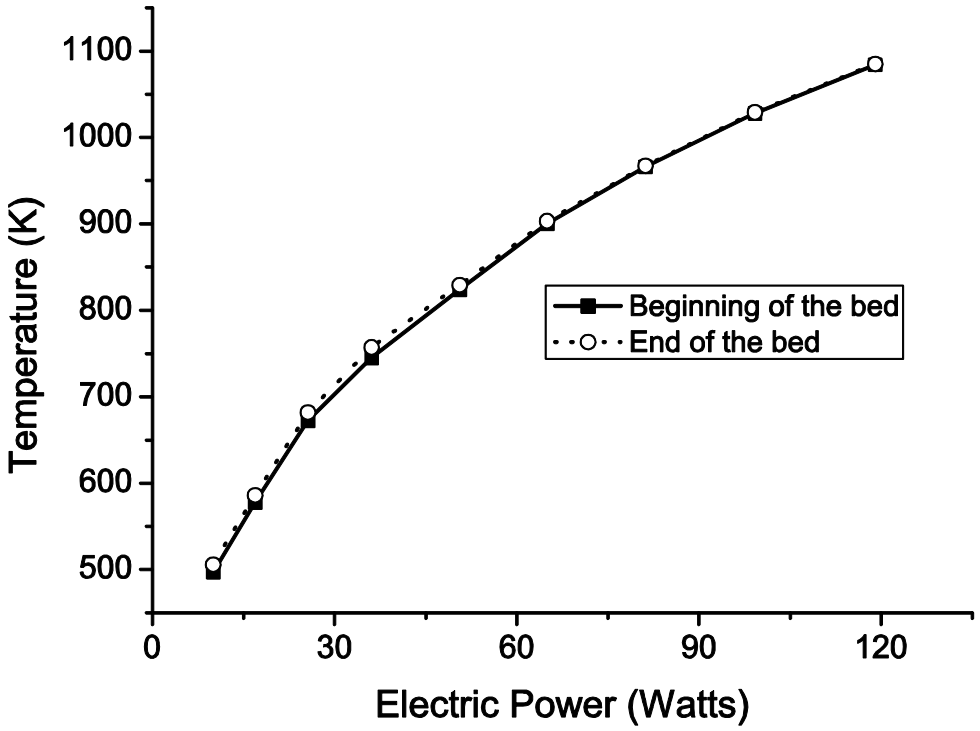

Figure 2 Electric Power vs Temperature for a 15000h^{-1} space velocity in a 1mm-diameter capillary with a 0.025mm wall thickness. This measurement was achieved using thermocouples inserted at both ends of the 8mm bed.

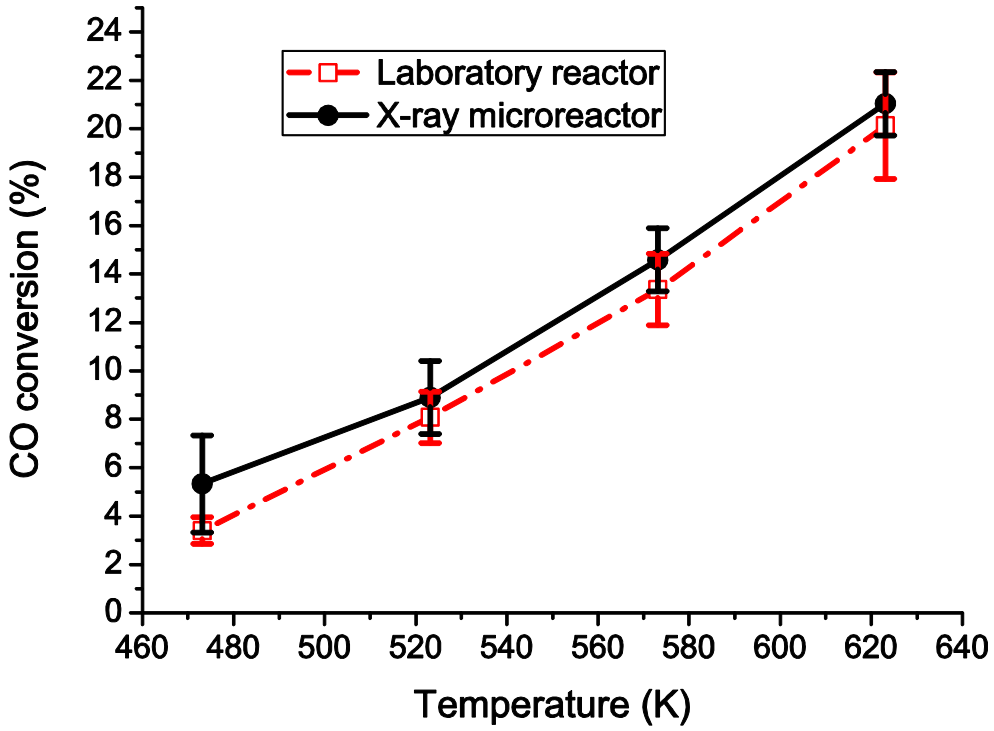

Figure 3 A comparison between the CO conversion for the water gas shift reaction of a standard laboratory reactor and that of the Aluminum X-ray microreactor using a 10 wt.%Cu in 12 wt.%CeO_2/Al_2O_3 reforming catalyst as a function of temperature. Four measures are taken at four different temperatures: 473, 523, 573 and 623 K, the errors are derived from the experimental results.

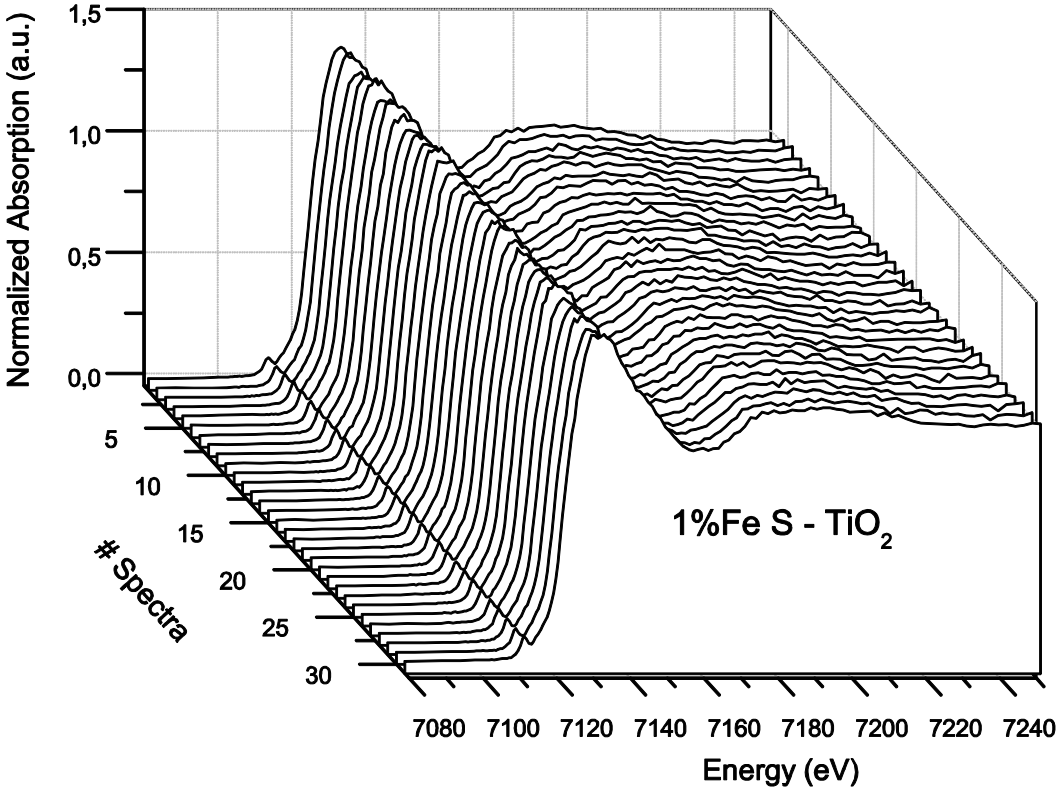

Figure 4 Fe K-edge XANES spectra obtained in BM23 by fluorescence mode, measured in between 300 up to 473K.

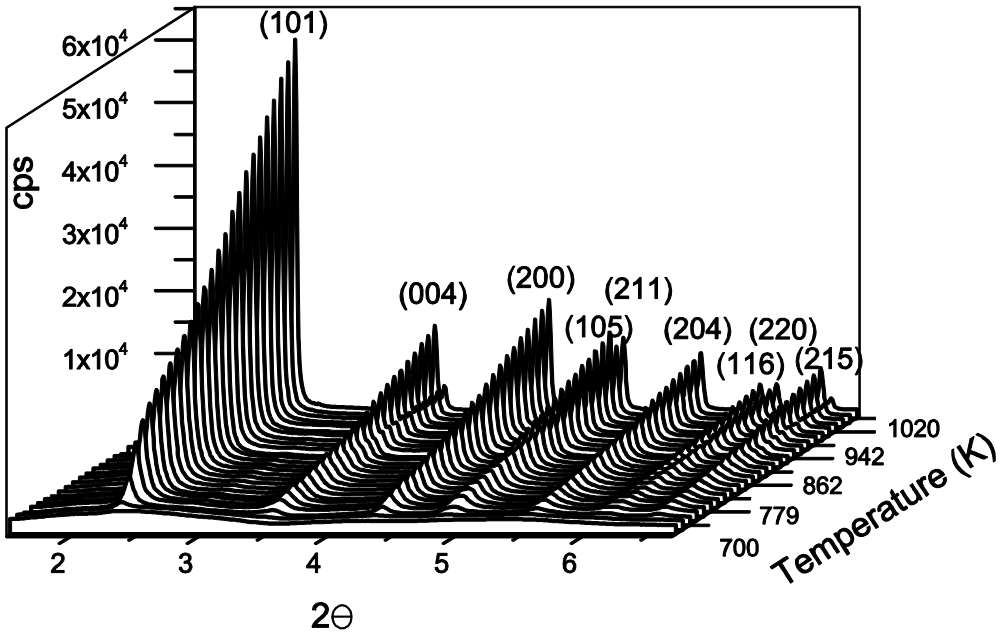

Figure 5 XRD diffractograms of TiO_2 sample taken during an ID15B calcination ramp.